

Rigidity–Stability Relationship in Interlocked Model Complexes Containing Phenylene-Ethyneylene-Based Disubstituted Naphthalene and Benzene

Il Yoon,[†] Diego Benítez,[†] Ognjen Š. Miljanic,^{†,‡} Yan-Li Zhao,[†] Ekaterina Tkatchouk,[§] William A. Goddard III,[§] and J. Fraser Stoddart^{*,†,‡}

Department of Chemistry and Biochemistry, University of California, Los Angeles, 405 Hilgard Avenue, Los Angeles, California 90095, Department of Chemistry, Northwestern University, 2145 Sheridan Road, Evanston, Illinois 60208, and Materials and Process Simulation Center, California Institute of Technology, 1200 East California Boulevard, Pasadena, California 91125

Received October 3, 2008; Revised Manuscript Received January 6, 2009

ABSTRACT: Structural rigidity has been found to be advantageous for molecules if they are to find applications in functioning molecular devices. In the search for an understanding of the relationship between the rigidity and complex stability in mechanically interlocked compounds, the binding abilities of two π -electron-rich model compounds (**2** and **4**), where rigidity is introduced in the form of phenylacetylene units, toward the π -electron deficient tetracationic cyclophane, cyclobis(paraquat-*p*-phenylene) (**CBPQT**⁴⁺), were investigated. 1,4-Bis(2-(2-methoxyethoxy)ethoxy)-2,5-bis(2-phenylethynyl)benzene **2** and 1,5-bis(2-(2-methoxyethoxy)ethoxy)-2,6-bis(2-phenylethynyl)naphthalene **4** were synthesized, respectively, from the appropriate precursor dibromides **1** and **3** of benzene and naphthalene carrying two methoxyethoxyethoxy side chains. The rigid nature of the compounds **2** and **4** is reflected in the reduced stabilities of their 1:1 complexes with **CBPQT**⁴⁺. Binding constants for both **2** (100 M⁻¹) and **4** (140 M⁻¹) toward **CBPQT**⁴⁺ were obtained by isothermal titration microcalorimetry (ITC) in MeCN at 25 °C. Compounds **1–4** were characterized in the solid state by X-ray crystallography. The stabilization within and beyond these molecules is achieved by a combination of intra- and intermolecular [C–H···O], [C–H···π], and [π–π] stacking interactions. The diethyleneglycol chains present in compounds **1–4** are folded as a consequence of both intra- and intermolecular hydrogen bonds. The preorganized structures in both precursors **1** and **3** are repeated in both model compounds **2** and **4**. In the structures of compounds **2** and **4**, the geometry of the rigid backbone is different—the two terminal phenyl groups are twisted with respect to the central benzenoid ring in compound **2** and roughly perpendicular to the plane central naphthalene core in compound **4**. To understand the significantly decreased stabilities of these complexes toward rigid guest molecules, relative to more flexible systems, we performed density functional theory (DFT) calculations using the newly developed M06-suite of density functionals. We conclude that the reduced binding abilities are a consequence of electronic and not steric factors, originating from the extended delocalization of the aromatic system.

Introduction

Certain π -electron-rich ring systems, such as 1,5-disubstituted dioxy naphthalene (DNP)¹ or 1,4-disubstituted dioxy benzene (HQ),² are readily encircled by the π -electron deficient tetracationic cyclophane, cyclobis(paraquat-*p*-phenylene) (**CBPQT**⁴⁺).³ These donor–acceptor pairs have been employed widely as components of mechanically interlocked molecules (MIMs), rotaxanes and catenanes, which have in turn found applications in functioning molecular devices.⁴ Addition of the oligo(ethyleneglycol) chains to the DNP and HQ-containing dumbbell-shaped components enhances their binding affinity toward the **CBPQT**⁴⁺ ring because of increased [C–H···O] interactions relative to the unsubstituted systems.^{1r,y}

Introduction of rigidity into these donors, e.g., through the incorporation of ethyneylene units, could be advantageous in the design of the functioning molecular devices⁴ because it would limit the number of co-conformations that a donor–acceptor couple can adopt in condensed media. Furthermore, structural rigidity has an advantage in switching processes^{1q,y} with the absence of back-folding⁶ to interact with the free recognition

sites in bistable systems and resulting in the development of molecular nanotechnology.⁷

Previously, we investigated the structure–stability relationship in the complexes containing carbonyl ester groups located along the polyether chains, known as pseudorotaxanes, to reveal that subtle structural changes through varying the location of the carbonyl ester afforded significant differences in the hydrogen bonding interactions, resulting²ⁱ in dramatic changes in the magnitudes of their association constants (K_a). In this paper, we report on the design and synthesis of rigid DNP- and HQ-containing model compounds. We follow with a discussion of their crystal structures that provide an understanding of the structural effects of introduced rigidity, as well as the reflected stability in their complexes with **CBPQT**⁴⁺.

Density functional theory (DFT) has been a popular computational tool^{10,8} in the designing and understanding of MIMs. We reported⁹ recently that the M06-suite of density functionals provides a better description for the structural, optical and binding properties of MIMs and their precursor complexes. Here, we use the same theoretical methodology to help us understand the origin of the decreased binding of interpenetrating rigid model complexes.

Experimental Section

Materials and Methods. All reagents were purchased from Aldrich and used without further purification. Cyclobis(paraquat-*p*-phenylene)-tetrakis(hexafluorophosphate) (**CBPQT**·4PF₆)³ was prepared according to literature procedures. Thin layer chromatography (TLC) was

* Corresponding author. E-mail: stoddart@northwestern.edu. Tel: (847) 491-3793. Fax: (847) 491-1009.

[†] University of California, Los Angeles.

[‡] Northwestern University.

[§] California Institute of Technology.

^y Present address: Department of Chemistry, University of Houston, 136 Fleming Building, Houston, Texas 77204-5003.

Table 1. Crystallographic Data for 1–4

	1	2	3	4
formula	C ₁₆ H ₂₄ Br ₂ O ₆	C ₃₂ H ₃₄ O ₆	C ₂₀ H ₂₆ Br ₂ O ₆	C ₃₆ H ₃₆ O ₆
<i>M</i>	472.17	514.59	522.23	564.65
cryst syst	monoclinic	triclinic	monoclinic	monoclinic
space group	<i>P</i> 2 ₁ / <i>n</i>	<i>P</i> 1̄	<i>P</i> 2 ₁ / <i>c</i>	<i>P</i> 2 ₁ / <i>n</i>
<i>a</i> (Å)	4.412(1)	9.675(2)	9.958(2)	7.634(1)
<i>b</i> (Å)	10.789(2)	10.145(3)	15.036(2)	19.513(2)
<i>c</i> (Å)	19.172(3)	14.934(4)	7.499(1)	10.643(1)
α (deg)	90	97.226(4)	90	90
β (deg)	93.731(2)	96.570(5)	93.717(3)	93.801(1)
γ (deg)	90	94.312(4)	90	90
<i>V</i> (Å ³)	910.7(2)	1438.6(6)	1120.5(3)	1581.9(2)
<i>Z</i>	2	2	2	2
<i>D</i> _c (g cm ⁻³)	1.722	1.188	1.626	1.185
<i>F</i> (000)	476	548	580	600
μ(Mo Kα)/mm ⁻¹	4.479	0.081	3.652	0.080
GOF on <i>F</i> ²	1.022	1.111	0.859	1.075
<i>R</i> ₁ and <i>wR</i> ₂ [<i>I</i> > 2σ(<i>I</i>)]	0.0225, 0.0489	0.1123, 0.3766	0.0402, 0.0960	0.0432, 0.1192
<i>R</i> ₁ and <i>wR</i> ₂ (all data)	0.0302, 0.0513	0.2853, 0.4435	0.0881, 0.1089	0.0693, 0.1330
(Δρ)max and (Δρ)min (e Å ⁻³)	0.494, -0.279	0.368, -0.264	0.365, -0.483	0.192, -0.168

Table 2. Selected Bond Lengths (Å), Angles (deg), and Torsion Angles (deg) for 1–4

	compd 1				
Br—C(1) O(1)—C(4)—C(5)—O(2)	1.894(2) 72.21(16)	O(1)—C(3) O(2)—C(6)—C(7)—O(3)	1.364(2) 69.87(17)	C(3)—O(1)—C(4) C(8)—O(3)—C(7)—C(6)	117.52(12) -174.19(14)
compd 2					
O(1)—C(1) C(15)—C(16)	1.370(7) 1.190(7)	O(4)—C(4) C(1)—O(1)—C(23)	1.365(7) 117.3(4)	C(7)—C(8) C(4)—O(4)—C(28)	1.185(7) 118.4(4)
O(1)—C(23)—C(24)—O(2) O(4)—C(28)—C(29)—O(5)	71.5(6) -69.6(6)			O(2)—C(25)—C(26)—O(3) O(5)—C(30)—C(31)—O(6)	64.3(8) -66.7(8)
C(27)—O(3)—C(26)—C(25)	-178.6(6)			C(32)—O(6)—C(31)—C(30)	175.6(6)
compd 3					
Br—C(3) O(1)—C(6)—C(7)—O(2)	1.891(3) -73.8(3)	O(1)—C(4) O(2)—C(8)—C(9)—O(3)	1.371(3) 64.8(4)	C(4)—O(1)—C(6)	115.90(19)
compd 4					
O(1)—C(10) O(1)—C(14)—C(15)—O(2)	1.3751(14) -69.62(15)	C(7)—C(8) O(2)—C(16)—C(17)—O(3)	1.1934(17) 178.70(12)	C(10)—O(1)—C(14)	115.05(10)

performed on silica gel 60 F254 (E. Merck). The plates were inspected by UV light and, if required, developed in I₂ vapor. Column chromatography was performed on silica gel 60F (Merck 9385, 0.040–0.063 mm). Melting points were recorded on an Electrothermal 9100 instrument in open capillary tubes and are uncorrected. Routine nuclear magnetic resonance (NMR) spectra were recorded at 25 °C on a Bruker Avance 500 and 400 spectrometers, with working frequencies of 500 and 400 MHz for ¹H, and 125 and 100 MHz for ¹³C nuclei, respectively. Chemical shifts are quoted in ppm on the δ scale and coupling constants (*J*) are expressed in Hertz (Hz). Samples for ¹H NMR spectroscopic investigations were prepared using solvents purchased from Cambridge Isotope Laboratories. All chemical shifts are reported relative to the residual solvent peak. The full assignment of the ¹H NMR signals was performed using 2D COSY (correlation spectroscopy) and ROESY (rotating-frame Overhauser enhancement spectroscopy) experiments. Matrix-assisted laser-desorption/ionization time-of-flight mass spectrometry (MALDI-time-of-flight MS) was performed on an IonSpec 4.7 T Ultima Fourier transform mass spectrometer, utilizing a 2,5-dihydroxybenzoic acid (DHB) matrix. High-resolution electrospray mass spectrometry (HRMS) was performed on an Applied Biosystems Q-STAR Elite Quad-TOF instrument.

1,4-Dibromo-2,5-bis(2-(2-methoxyethoxy)ethoxy)benzene (1). KOH (1.88 g, 33.6 mmol) was dissolved in anhydrous Me₂SO (20 mL), forming a yellow solution, which was stirred for 10 min and degassed at room temperature. 2,5-Dibromobenzene-1,4-diol (1.00 g, 3.73 mmol) and 1-bromo-2-(2-methoxyethoxy)ethane (2.73 g, 14.9 mmol) were added to the solution, causing a color change to dark brown. After 3 h of stirring, the reaction mixture was poured into ice H₂O (500 mL), and stirred until it reached room temperature. After extraction with Et₂O, the solvent was evaporated and the residue was purified by column chromatography (SiO₂: 50% EtOAc/Hexane) to afford **1** as a white solid (1.4 g, 79%). **1**: mp 49–51 °C; HRMS calcd for C₁₆H₂₅Br₂O₆, 471.0017 [M + H]⁺; found, 471.0337; calcd for C₁₆H₂₄NaBr₂O₆,

492.9837 [M + Na]⁺; found, 492.9829. MALDI-TOF MS *m/z* 472 [M]⁺. ¹H NMR (500 MHz, CD₃COCD₃): δ 7.31 (2H, s), 4.16 (4H, t, *J* = 5 Hz), 3.80 (4H, t, *J* = 5 Hz), 3.65 (4H, t, *J* = 5 Hz), 3.47 (4H, t, *J* = 5 Hz), 3.27 (6H, s). ¹³C NMR (125 MHz, CDCl₃): δ 150.2, 118.7, 110.7, 71.7, 70.4, 69.9, 69.2, 57.9.

1,4-Bis(2-(2-methoxyethoxy)ethoxy)-2,5-bis(2-phenylethynyl)benzene (2). Compound **1** (700 mg, 1.48 mmol), phenylacetylene (0.45 g, 4.44 mmol), PdCl₂(PPh₃)₂ (40 mg, 0.057 mmol), CuI (100 mg, 0.525 mmol), and PPh₃ (40 mg, 0.153 mmol) were dissolved in NEt₃ (45 mL), causing a color change to dark brown, before the reaction mixture was heated under reflux for 3 days. After extraction with CH₂Cl₂, the solvent was evaporated and the residue was purified by column chromatography (SiO₂: 50% EtOAc/CH₂Cl₂) to afford **2** as a pale yellow solid (300 mg, 39%). **2**: mp 76–79 °C; HRMS calcd for C₃₂H₃₅O₆, 515.2433 [M + H]⁺; found, 515.2848; calcd for C₃₂H₃₄NaO₆, 537.2253 [M + Na]⁺; found, 537.2248. MALDI-TOF MS *m/z* 514 [M]⁺, 537 [M + Na]⁺. ¹H NMR (500 MHz, CDCl₃): δ 7.57 (4H, d, *J* = 8 Hz), 7.40–7.39 (6H, m), 7.10 (2H, s), 4.27 (4H, t, *J* = 5 Hz), 3.98 (4H, t, *J* = 5 Hz), 3.86 (4H, t, *J* = 5 Hz), 3.58 (4H, t, *J* = 5 Hz), 3.41 (6H, s). ¹³C NMR (125 MHz, CDCl₃): δ 153.5, 131.4, 128.2, 123.2, 117.3, 114.1, 94.9, 85.6, 82.9, 71.9, 71.0, 69.6, 69.5, 58.9.

2,6-Dibromo-1,5-bis(2-(2-methoxyethoxy)ethoxy)naphthalene (3). KOH (4.76 g, 84.8 mmol) was dissolved in anhydrous Me₂SO (60 mL), causing a color change to yellow. The reaction mixture was stirred for 10 min and degassed at room temperature. 2,6-Dibromonaphthalene-1,5-diol (3.0 g, 9.44 mmol) and 1-bromo-2-(2-methoxyethoxy)ethane (6.12 g, 33.4 mmol) were added to the solution, causing a color change to dark brown. After 16 h of stirring, the reaction mixture was poured into ice H₂O (500 mL), and stirred until it reached room temperature. After extraction with EtOAc, the solvent was evaporated and the residue was purified by column chromatography (SiO₂: 50% EtOAc/Hexane) to afford **3** as a pale yellow solid (2.71 g, 55%). **3**: mp 56–58 °C; HRMS calcd for C₂₀H₂₇Br₂O₆, 521.0174 [M + H]⁺; found, 521.0509;

Table 3. Hydrogen Bonds and C–H \cdots π Interaction Geometries (\AA , deg) for 1–4

Compd 1					
D–H \cdots A	D–H (\AA)	H \cdots A (\AA)	D \cdots A (\AA)	D–H \cdots A (deg)	symmetry
C(6)–H(6A) \cdots O(1)	1.0	2.6	3.2	120	
C(5)–H(5B) \cdots O(1) ⁱ	1.0	2.8	3.4	120	$-1 + x, y, z$
C(4)–H(4B) \cdots O(2) ⁱⁱ	1.0	2.7	3.3	123	$-x, 2 -y, 1 -z$
D–H \cdots π	D–H (\AA)	H \cdots π (\AA)	D–H \cdots π (deg)		symmetry
C(4)–H(4A) \cdots π (C1–C3A) ⁱ	1.0	2.9	135		$-1 + x, y, z$
Compd 2					
D–H \cdots A	D–H (\AA)	H \cdots A (\AA)	D \cdots A (\AA)	D–H \cdots A (deg)	symmetry
C(25)–H(25A) \cdots O(1)	1.0	2.5	3.1	121	
C(30)–H(30B) \cdots O(4)	1.0	2.6	3.2	120	
C(28)–H(28A) \cdots O(5) ⁱⁱⁱ	1.0	2.5	3.3	145	$1 -x, -y, 1 -z$
D–H \cdots π	D–H (\AA)	H \cdots π (\AA)	D–H \cdots π (deg)		symmetry
C(10)–H(10) \cdots π (C17–C22) ^{iv}	1.0	3.1	128		$1 -x, 1 -y, 1 -z$
Compd 3					
D–H \cdots A	D–H (\AA)	H \cdots A (\AA)	D \cdots A (\AA)	D–H \cdots A (deg)	symmetry
C(1)–H(1) \cdots O(2) ^v	1.0	2.6	3.5	153	$1 -x, -y, -z$
C(9)–H(9A) \cdots O(3) ^{vi}	1.0	2.7	3.6	148	$x, 3/2 -y, -1/2 +z$
D–H \cdots π	D–H (\AA)	H \cdots π (\AA)	D–H \cdots π (deg)		symmetry
C(7)–H(7B) \cdots π (C1–C5A) ^{vii}	1.0	3.0	141		$x, y, -1 +z$
Compd 4					
D–H \cdots A	D–H (\AA)	H \cdots A (\AA)	D \cdots A (\AA)	D–H \cdots A (deg)	symmetry
C(12)–H(12) \cdots O(2)	1.0	2.6	3.4	146	
C(5)–H(5) \cdots O(3) ^{viii}	1.0	2.5	3.4	159	$1 + x, y, -1 +z$
D–H \cdots π	D–H (\AA)	H \cdots π (\AA)	D–H \cdots π (deg)		symmetry
C(16)–H(16A) \cdots π (C9 ^{ix} –C13 ^x)	1.0	3.0	143	$-1 + x, y, z; 2 -x, 1 -y, 1 -z$	
C(17) ^{xi} –H(17B) ^{xii} \cdots π (C1–C6)	1.0	2.8	138	$3 -x, 1 -y, -z$	
C(15)–H(15A) \cdots π (C1–C6) ^{xii}	1.0	3.0	124	$5/2 -x, -1/2 +y, 3/2 -z$	

calcd for $C_{20}H_{26}NaBr_2O_6$, 542.9994 [M + Na] $^+$; found, 543.0359. MALDI-TOF MS *m/z* 545 [M + Na] $^+$. ^1H NMR (500 MHz, CD₃COCD₃): δ 8.05 (2H, d, *J* = 9 Hz), 7.65 (2H, d, *J* = 9 Hz), 4.23 (4H, t, *J* = 5 Hz), 3.84 (4H, t, *J* = 5 Hz), 3.66 (4H, t, *J* = 5 Hz), 3.52 (4H, t, *J* = 5 Hz), 3.31 (6H, s). ^{13}C NMR (125 MHz, CDCl₃): δ 152.3, 130.8, 130.1, 120.2, 113.3, 73.4, 71.7, 70.3, 69.8, 58.0.

1,5-Bis(2-(2-methoxyethoxy)ethoxy)-2,6-bis(2-phenylethynyl)naphthalene (4). Compound 3 (850 mg, 1.63 mmol), phenylacetylene (0.50 g, 4.89 mmol), PdCl₂(PPh₃)₂ (70 mg, 0.098 mmol), CuI (100 mg, 0.525 mmol), and PPh₃ (60 mg, 0.229 mmol) were dissolved in NEt₃ (80 mL), causing a color change to dark brown, before the reaction mixture was heated under reflux for 3 days. After extraction with EtOAc, the solvent was evaporated and the residue was purified by column chromatography (SiO₂: 30% EtOAc/Hexane) to afford 4 as a pale yellow solid (383 mg, 42%). 4: mp 47–49 °C; HRMS calcd for C₃₆H₃₇O₆, 565.2590 [M + H] $^+$; found, 565.3025; calcd for C₃₆H₃₆NaO₆, 587.2410 [M + Na] $^+$; found, 587.2811. MALDI-TOF MS *m/z* 564 [M] $^+$, 587 [M + Na] $^+$. ^1H NMR (400 MHz, CDCl₃): δ 8.05 (2H, d, *J* = 8 Hz), 7.61–7.59 (4H, m), 7.56 (2H, d, *J* = 8 Hz), 7.39–7.37 (6H, m), 4.58 (4H, t, *J* = 5 Hz), 3.96 (4H, t, *J* = 5 Hz), 3.75 (4H, t, *J* = 5 Hz), 3.59 (4H, t, *J* = 5 Hz), 3.41 (6H, s). ^{13}C NMR (100 MHz, CDCl₃): δ 157.0, 131.5, 129.8, 129.4, 128.5, 128.4, 123.3, 118.4, 112.9, 95.5, 86.6, 73.5, 72.1, 70.7, 70.6, 59.2.

Isothermal Titration Microcalorimetry (ITC) Investigation. The calorimetric titrations were performed on an isothermal titration microcalorimeter at the atmospheric pressure and 25 °C in MeCN. In each run, a solution of the model compound in a 0.250 mL syringe was sequentially injected with stirring at 300 rpm into a solution of **CBPQT** \cdot 4PF₆ in the sample cell (1.4 mL volume). Each titration experiment involved 29–59 successive injections. A control experiment was performed to determine the heat of dilution by injecting a solution of the model compound into a solution without the **CBPQT** \cdot 4PF₆. The dilution enthalpy was subtracted from the apparent enthalpy obtained

in each titration run, and the net reaction enthalpy was analyzed by using the “one set of binding sites” model. The Origin software (Microcal) was employed to determine binding constants (*K*_S) with the standard derivations simultaneously on the basis of the scatter of data points from a single titration experiment.

Crystallographic Investigation. The data (Tables 1 and 2) were processed using the program SAINT (Bruker Analytical X-Ray Instrument Inc., Madison, WI) to give the structure factors. The structures were solved by direct methods and refined by full-matrix least-squares against |F²|. Absorption corrections were based on multiple and symmetry-equivalent reflections in the data sets using the SADABS program (G. M. Sheldrick, Göttingen University, Germany). All non-hydrogen atoms were refined anisotropically. Hydrogen atoms were treated as idealized contributions. Scattering factors and anomalous dispersion coefficients are contained in the SHELXTL 6.12 program library (G. M. Sheldrick, Madison, WI). CCDC-683613 (**1**), CCDC-677835 (**2**), CCDC-683614 (**3**), and CCDC-677836 (**4**) contain the supplementary crystallographic data for this paper. These data can be obtained free of charge from the Cambridge Crystallographic Data Centre via www.ccdc.cam.ac.uk/data_request/cif.

Theoretical Investigation. Calculations were performed on all systems using density functional theory (DFT) with the M06-L, M06-HF and M06-L functionals,¹⁰ as implemented in Jaguar 7.0 (release 207).¹¹ The M06 functional is a new hybrid meta-GGA exchange-correlation functional that leads to impressive accuracy for a very large validation set of systems, including van der Waals dimers, reactions, and transition metal complexes. Starting with structures from crystallographic data we optimized the geometry using the 6–31+G** basis set with the M06-L functional in the gas phase. Single point energies were calculated using the M06 functional and the 6–311++G** basis set. Solvent corrections were based on single point self-consistent

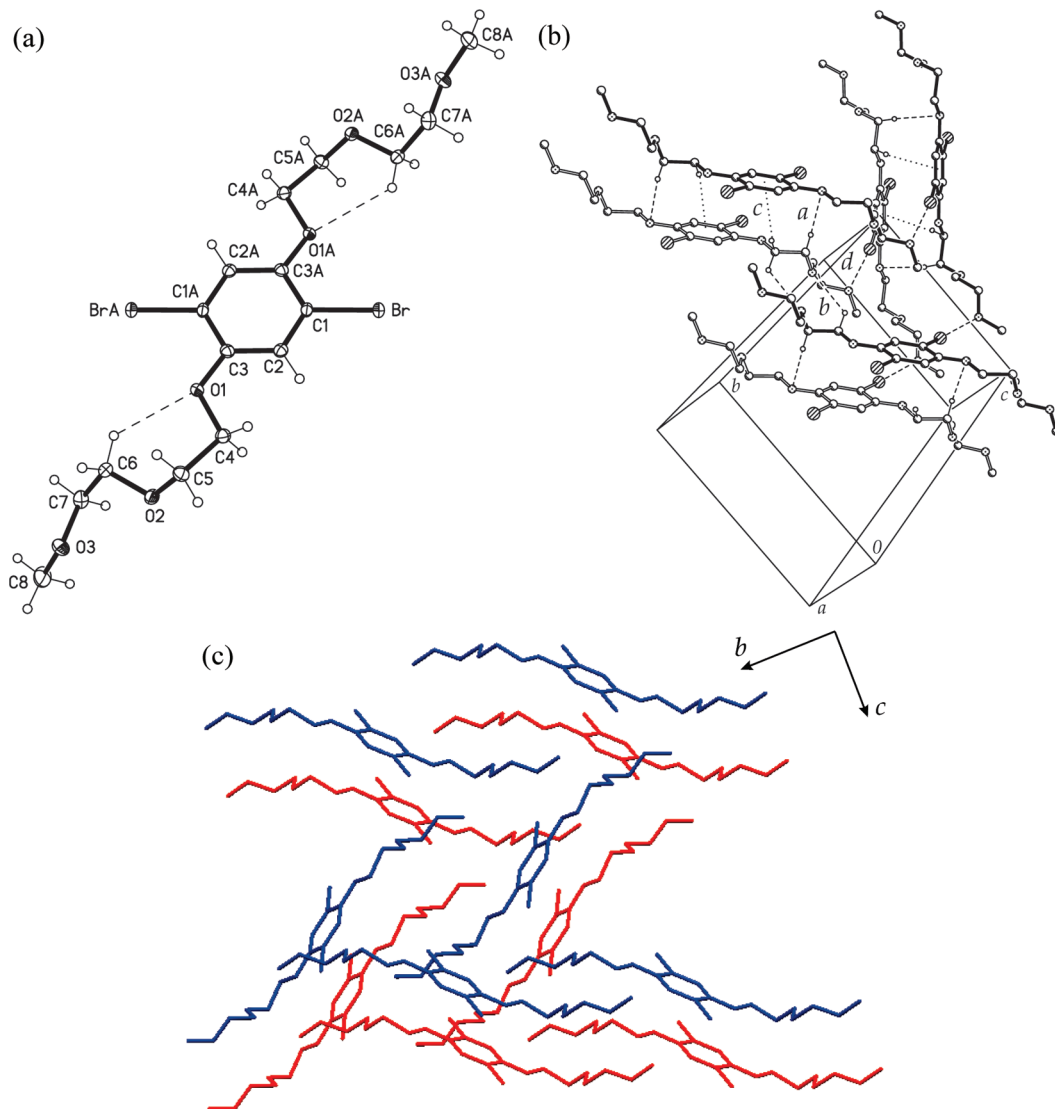


Figure 1. (a) ORTEP diagram of **1** with the atomic labeling scheme (50% probability), showing intramolecular $[C-H \cdots O]$ interactions. (b) Unit cell drawing of the packing arrangement for **1**, showing hydrogen bonds, $[Br \cdots O]$ contacts, and $[C-H \cdots \pi]$ interactions. $[C-H \cdots O]$ interaction geometries $\{[X \cdots O], [H \cdots O]\}$ distances (\AA), and $[X-H \cdots O]$ angles (deg): (a) 3.4, 2.8, 120; (b) 3.3, 2.7, 123. The $[H \cdots \pi]$ distances (\AA) and $[C-H \cdots \pi]$ angles (deg) for the $[C-H \cdots \pi]$ interactions are (c) 2.9, 135. (d) $[Br \cdots O]$ contact (\AA): 3.2. The H atoms except hydrogen bonds and $[C-H \cdots \pi]$ interactions were omitted for clarity. (c) In the packing structure of **1**, each layer is shown in same color.

Poisson–Boltzmann continuum solvation calculations for acetonitrile ($\epsilon = 37.5$, $R_0 = 2.18 \text{ \AA}$) using the PBF module in Jaguar.

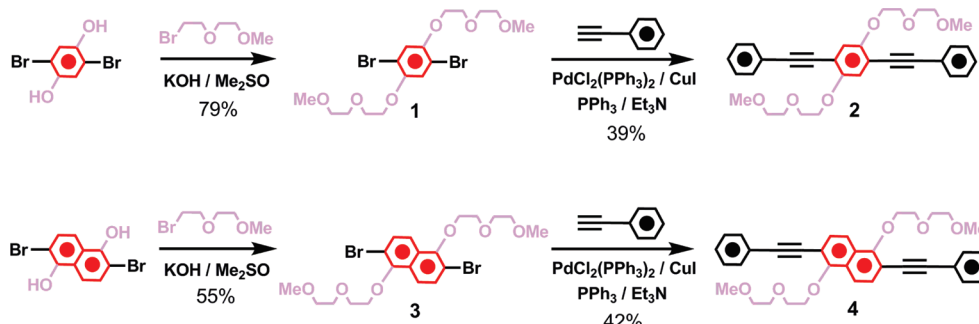
Results and Discussion

Syntheses. The routes to the synthesis of compounds are shown in Scheme 1. 1,4-Dibromo-2,5-bis(2-(2-methoxyethoxy)ethoxy)benzene (**1**) has been previously synthesized by Wegner et al.¹² We prepared compound **1**, as a precursor to 1,4-bis(2-(2-methoxyethoxy)ethoxy)-2,5-bis(2-phenylethylnyl)benzene (**2**), by reacting¹³ 2,5-dibromobenzene-1,4-diol and 1-bromo-2-(2-methoxyethoxy)ethane in the presence of KOH/Me₂SO at 25 °C. 2,6-Dibromo-1,5-bis(2-(2-methoxyethoxy)ethoxy)naphthalene (**3**), as a precursor to 1,5-bis(2-(2-methoxyethoxy)ethoxy)-2,6-bis(2-phenylethylnyl)naphthalene (**4**), was synthesized by an extension of the synthetic method used to prepare **1**, starting with 2,6-dibromonaphthalene-1,5-diol. Compounds **2** and **4** were prepared as model systems for the rigid HQ- and DNP-containing dumbbell-shaped compounds. Their central HQ and DNP units are substituted with both diethyleneglycol (DEG) chains and rigid phenylene-ethynylene groups. Compounds **2**

and **4** were synthesized by carrying out Sonogashira¹⁴ couplings of **1** and **3**, respectively, with phenylacetylene. Compounds **1–4** were characterized by NMR spectroscopy and mass spectrometry.

ITC Investigation. Measurements of the binding abilities of **CBPQT**⁴⁺ toward the different guests were performed by isothermal titration microcalorimetry (ITC) in MeCN at 25 °C. The binding constants (K_S) of **CBPQT**·4PF₆ with both compounds **2** and **4** were ca. 100 M⁻¹ and 140 M⁻¹, respectively. The binding constant of **4** with **CBPQT**·4PF₆ was slightly higher than that of **2** because the DNP-containing dumbbell-shaped molecule has a higher binding ability than the HQ-containing one because of the stronger electron donor effect in DNP. The binding constants were significantly decreased compared with the more flexible dumbbell-shaped analogue molecules with absence of the phenylene-ethynylene, i.e., disubstituted DEG-DNP^{3b} and DEG-HQ²¹ were reported as ca. 7200 and 3800 M⁻¹, respectively, in MeCN at 25 °C. This result shows that the introduction of the rigid frameworks, decreased flexibility, into **2** and **4** allows changing an environment of the $[C-H \cdots O]$ interactions between the oxygen atoms in **2** and **4**.

Scheme 1. Syntheses of 1–4



and the hydrogen atoms on the bipyridinium units of the CBPQT⁴⁺ ring, leading to a decrease in stabilization provided by the [C—H···O] interactions.

Structural Investigations. Crystallographic data and selected bond lengths, angles, and torsion angles for **1–4** are summarized in Tables 1 and 2, respectively. The hydrogen bonds and [C—H···π] interaction geometries for **1–4** are summarized in Table 3.

Structural Investigation of 1. Colorless block-shaped single crystals of **1**, suitable for X-ray crystallography, were obtained by slow evaporation of a CH₂Cl₂/hexane solution. Figure 1a

shows an ORTEP representation of compound **1** which crystallizes in a monoclinic *P*2₁/*n* unit cell, adopting a centrosymmetric geometry with an inversion center on the HQ unit; the stabilization within and beyond the molecule is achieved by intra- and intermolecular hydrogen bonds, and [C—H···π] interactions. Each DEG chain adopts an S-shaped conformation through two gauche arrangements [O(1)—C(4)—C(5)—O(2) 72°, O(2)—C(6)—C(7)—O(3) 70°] because of the intramolecular [C—H···O] interactions⁵ (Figure 1a) between the oxygen atom (O1) in the DEG chain and the proton of the DEG carbon (C6), intermolecular [C—H···O] interactions (Figure 1b-a,b) between

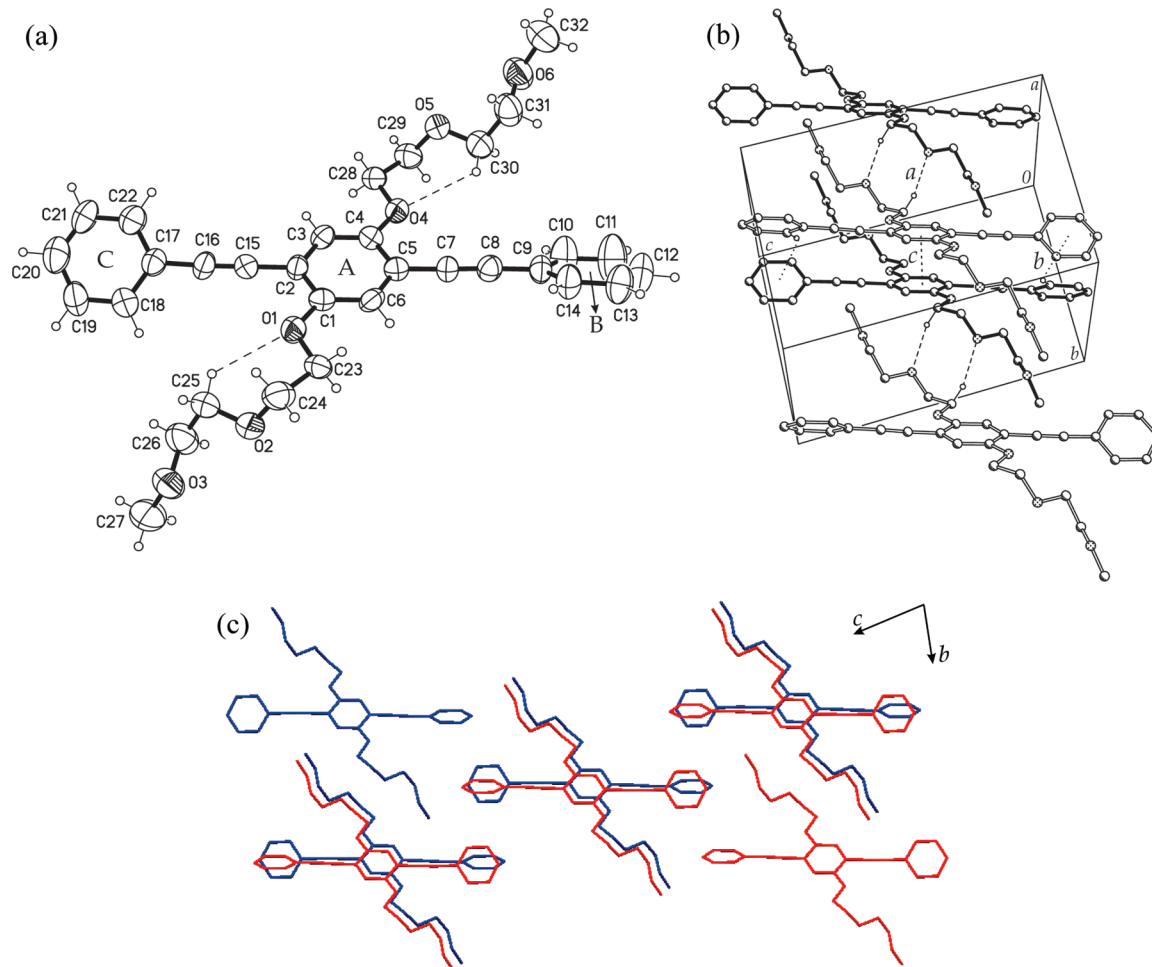


Figure 2. (a) ORTEP diagram of **2** with the atomic labeling scheme (50% probability), showing intramolecular [C—H···O] interactions. (b) Unit cell drawing of the packing arrangement for **2**, showing hydrogen bonds, [C—H···π] interactions, and [π···π] stacking interactions. [C—H···O] interaction geometries {X···O}, [H···O] distances (Å), and [X—H···O] angles (deg): (a) 3.3, 2.5, 145. The [H···π] distances (Å) and [C—H···π] angles (deg) for the [C—H···π] interactions are (b) 3.1, 128. (c) Face-to-face [π···π] stacking interactions: 3.5 Å. The H atoms except hydrogen bonds and [C—H···π] interactions were omitted for clarity. (c) In the packing structure of **2**, each layer is shown in the same color.

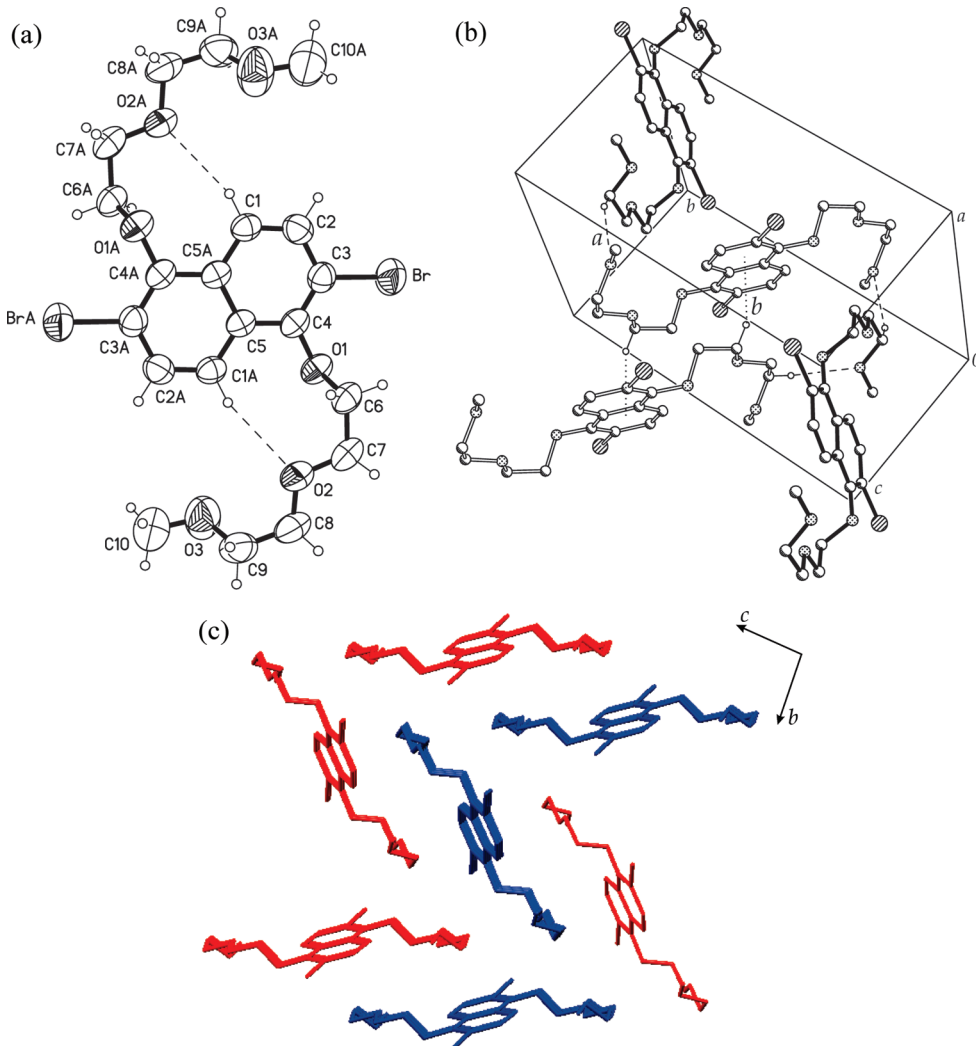


Figure 3. (a) ORTEP diagram of **3** with the atomic labeling scheme (50% probability), showing intramolecular $[C-H \cdots O]$ interactions. (b) Unit-cell drawing of the packing arrangement for **3**, showing hydrogen bonds and $[C-H \cdots \pi]$ interactions. $[C-H \cdots O]$ interaction geometries $\{[X \cdots O], [H \cdots O]\}$ distances (\AA), and $[X-H \cdots O]$ angles (deg): (a) 3.6, 2.7, 148. The $[H \cdots \pi]$ distances (\AA) and $[C-H \cdots \pi]$ angles (deg) for the $[C-H \cdots \pi]$ interactions are (b) 3.0, 141. The H atoms except hydrogen bonds and $[C-H \cdots \pi]$ interactions were omitted for clarity. (c) In the packing structure of **3**, each layer is shown in the same color.

the oxygen atoms (O1, O2) and the protons of the DEG carbons (C5, C4) in neighboring molecules, and $[C-H \cdots \pi]$ interactions^{12,15} (Figure 1b-c) between the central HQ unit and the proton of the DEG carbon (C4), resulting in total length of 18.1 \AA between two termini of methyl carbons (C8, C8A) in DEG chains. Interestingly, the oxygen atom (O3) has a $[Br \cdots O]$ contact of 3.19 \AA (Figure 1b-d), which is shorter than the ranges (3.21–3.34 \AA) reported previously.¹⁶ In the packing structure, the continuous intermolecular $[C-H \cdots O]$ interactions and the $[Br \cdots O]$ contacts allow the zigzag type packed columns (Figure 1c) with a dihedral angle 78° between the central HQ planes in neighboring columns.

Structural Investigation of 2. Pale-yellow colored plate-shaped single crystals of **2**, suitable for X-ray crystallography, were obtained by slow evaporation of $\text{CH}_2\text{Cl}_2/\text{hexane/Et}_2\text{O}$ solution. Figure 2a shows an ORTEP representation of compound **2** which crystallizes in a triclinic $P\bar{1}$ unit cell, which has similar bond lengths for its HQ and ethynyl C–C bonds to its unsubstituted analogue 1,4-bis(phenylethyynyl)benzene,¹⁷ as well as the disubstituted analogue.¹⁸ Compound **2** adopts a noncentrosymmetric folded and twisted conformations; the stabilization within and beyond the molecule is achieved by intra- and

intermolecular hydrogen bonds, $[C-H \cdots \pi]$ interactions, and $[\pi-\pi]$ stacking interactions. Similarly in **1**, each DEG chain adopts an S-shaped conformation with gauche arrangements $[O(1)-C(23)-C(24)-O(2) 72^\circ, O(2)-C(25)-C(26)-O(3) 64^\circ, O(4)-C(28)-C(29)-O(5) -70^\circ, O(5)-C(30)-C(31)-O(6) -67^\circ]$ by the intramolecular $[C-H \cdots O]$ interactions (Figure 2a) between the oxygen atoms (O1, O4) in the DEG chains and the protons of the DEG carbons (C25, C30), intermolecular $[C-H \cdots O]$ interactions (Figure 2b-a) between the oxygen atoms (O5) and the protons of the DEG carbons (C28) in neighboring molecules, and $[C-H \cdots \pi]$ interactions (Figure 2b-b) between the terminal phenyl and the proton of the terminal phenyl carbon (C10), resulting in a total length of 17.7 \AA between two termini of methyl carbons (C27, C32) in DEG chains.

Interestingly, two terminal phenyl units are twisted with dihedral angles $[A \cdots B 30^\circ, A \cdots C 145^\circ]$ from the central HQ ring on the fully rigid conjugated framework with a length of 16.5 \AA by the intermolecular $[C-H \cdots \pi]$ interactions (Figure 2b-b). Otherwise, the central HQ ring has face-to-face $[\pi-\pi]$ stacking interactions^{12,19} ($C1-C6$) [distance: 3.5 \AA] in packing structure (Figure 2b-c and Figure 2c), which is more twisted

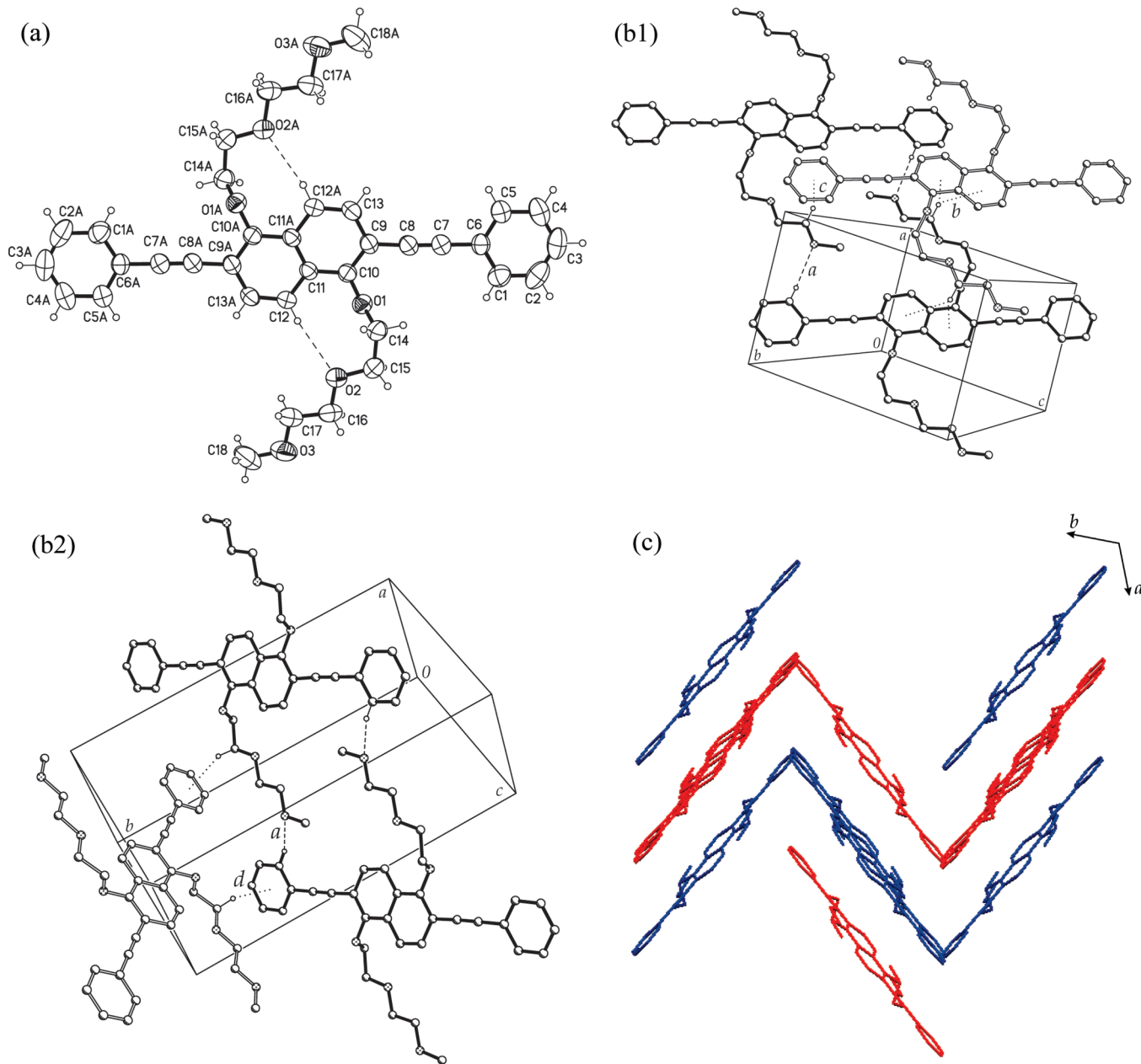


Figure 4. (a) ORTEP diagram of **4** with the atomic labeling scheme (50% probability), showing intramolecular [C–H \cdots O] interactions. (b) Unit cell drawing of the packing arrangement for **4**, showing hydrogen bonds and [C–H \cdots π] interactions. [C–H \cdots O] interaction geometries {[X \cdots O], [H \cdots O] distances (\AA), and [X–H \cdots O] angles ($^\circ$)}: (a) 3.4, 2.5, 159. The [H \cdots π] distances (\AA) and [C–H \cdots π] angles ($^\circ$) for the [C–H \cdots π] interactions are (b) 3.0, 143; (c) 2.9, 138; (d) 3.0, 124. The H atoms except hydrogen bonds and [C–H \cdots π] interactions were omitted for clarity. (c) In the packing structure of **4**, each layer is shown in same color.

than the analogue molecule¹⁸ (this structure was centrosymmetric with a dihedral angle 20°).

Structural Investigation of 3. Colorless plate-shaped single crystals of **3**, suitable for X-ray crystallography, were obtained by slow evaporation of CH₂Cl₂/hexane solution. Figure 3a shows an ORTEP representation of compound **3** which crystallizes in a monoclinic *P2₁/c* unit cell, adopting a centrosymmetric conformation with an inversion center on the DNP unit, and an S-shaped conformation; the stabilization within and beyond the molecule is achieved by intra- and intermolecular hydrogen bonds, and [C–H \cdots π] interactions. Each DEG chain adopts a folded conformation through two gauche arrangements [O(1)–C(6)–C(7)–O(2) –74°, O(2)–C(8)–C(9)–O(3) 65°] on account of the intramolecular [C–H \cdots O] interactions (Figure 3a) between the oxygen atom (O2) and the proton on the DNP

carbon (C1A), resulting in significantly shorter total length of 12.5 Å between two termini of methyl carbons (C10, C10A) in DEG chains than that in **1** (18.1 Å). The packing structure (Figure 3b) is stabilized by a combination of the continuous (a) intermolecular [C–H \cdots O] interactions (Figure 3b-a) between the oxygen atom (O3) and the proton of the DEG carbon (C9) and (b) the [C–H \cdots π] interactions (Figure 3b-b) between the proton of the DEG carbon (C7) and the DNP. There is no [Br \cdots O] contact shown in **3**. Similarly in **1**, the intermolecular [C–H \cdots O] interactions (Figure 3b-a) connect each columns to afford the zigzag type packed columns (Figure 3c) with a dihedral angle 84° between the central DNP planes in neighboring columns, a value that is slightly larger than that in **1**, between the DNP planes in neighboring columns.

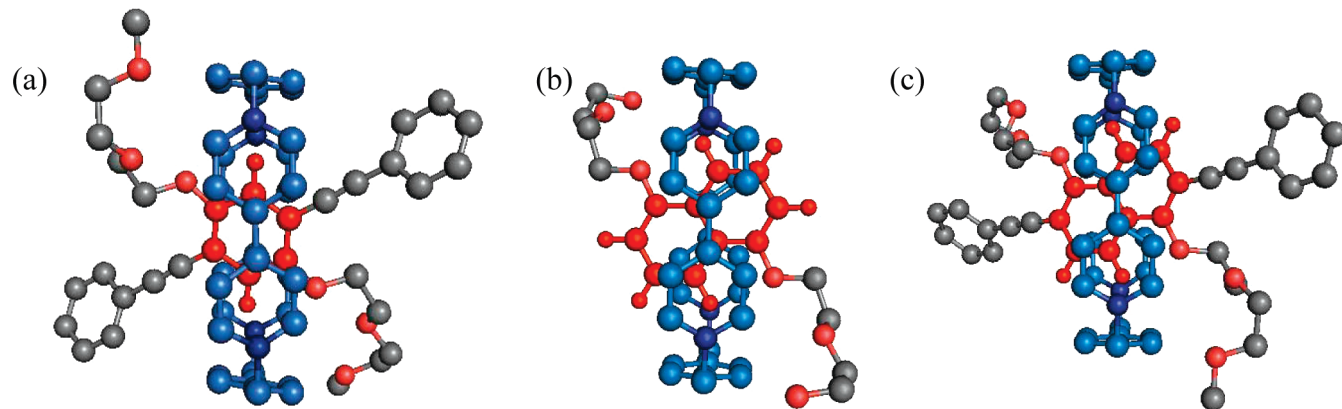


Figure 5. Top view of the M06-L/6-31+G** minimized superstructures (a) $2_{\text{2}}\text{CBPQT}^{4+}$, (b) DEG-DNP·CBPQT $^{4+}$, and (c) $4_{\text{2}}\text{CBPQT}^{4+}$.

Structural Investigation of 4. Yellow-colored cut-prism-shaped single crystals of **4** were obtained by slow evaporation of $\text{CH}_2\text{Cl}_2/\text{hexane}$ solution. Figure 4a shows an ORTEP representation of compound **4** which crystallizes in a monoclinic $P2_1/n$ unit cell, adopting a centrosymmetric conformation with an inversion center in the DNP unit. Similarly in **3**, each DEG chain associated with the DNP unit adopts an S-shaped conformation; the stabilization is achieved by a combination of (a) intramolecular [C–H \cdots O] interactions (Figure 4a) between the oxygen atom (O2) and the proton on the DNP carbon (C12), (b) intermolecular [C–H \cdots O] interactions (Figure 4b-a) between the oxygen atom (O3) and the proton of the DEG carbon (C5) in the same layer, and (c) [C–H \cdots π] interactions (Figure 4b-b,c,d) between the protons of the DEG carbons (C15, C17) and the terminal phenyl, as well as between the proton on the DEG carbon (C16) and the DNP. In addition, the intermolecular [C–H \cdots O] interactions and the [C–H \cdots π] interactions allow quite different environments between two DEG chains through gauche [O(1)–C(14)–C(15)–O(2) 70°] and anti [O(2)–C(16)–C(17)–O(3) 179°] arrangements, resulting in total length of 16.0 Å, between the termini of methyl carbons (C18, C18A) in DEG chains, which is significantly longer than that in **3** (12.5 Å). The terminal phenyl groups and DNP rings are planar to each other within 8°, as expected, resulting in a fully rigid conjugated framework with total length of 18.7 Å. Interestingly, **4** has no face-to-face [π – π] stacking interaction between the aromatic rings, otherwise the DNP unit and the two terminal phenyl units have interlayer [C–H \cdots π] interactions in the packing structure. Similarly in **1** and **3**, the intermolecular [C–H \cdots O] interactions connect each columns to afford the zigzag type packed columns (Figure 4c) with a

dihedral angle 91°, which is slightly larger than that in **3**, between the DNP planes in neighboring columns.

Theoretical Investigations. Structures for **2**, **4**, CBPQT $^{4+}$ and superstructures for $2_{\text{2}}\text{CBPQT}^{4+}$ and $4_{\text{2}}\text{CBPQT}^{4+}$ were calculated at the M06/6-311++G**//M06-L/6-31+G** level of theory. This method predicts a binding of $-27.7 \text{ kcal mol}^{-1}$ for $2_{\text{2}}\text{CBPQT}^{4+}$ and $-21.4 \text{ kcal mol}^{-1}$ for $4_{\text{2}}\text{CBPQT}^{4+}$ compared to $-6.6 \pm 0.8 \text{ kcal mol}^{-1}$ and $-3.9 \pm 1.1 \text{ kcal mol}^{-1}$ measured by ITC (see the Supporting Information). This comparison between experiment and theory shows that M06 overestimates the binding by 21.1 and 17.5 kcal mol $^{-1}$ for the formation of $2_{\text{2}}\text{CBPQT}^{4+}$ and $4_{\text{2}}\text{CBPQT}^{4+}$, respectively. This overestimate is in agreement with our recent report⁹ in which we showed that the binding predictions for a similar rigid pseudorotaxane with the same functional and basis set (M06/6-311++G**) were $\sim 22 \text{ kcal mol}^{-1}$ stronger than experiment.

To understand the significantly decreased stabilities of these complexes toward rigid guest molecules, relative to more flexible systems, we minimized the superstructure (Figure 5b) of disubstituted DEG-DNP with CBPQT $^{4+}$. Because there is no appreciable change in the relative positioning of the DNP unit with respect to CBPQT $^{4+}$ in comparison with the much stronger disubstituted DEG-DNP complex (structures b and c in Figure 5), it is unlikely that the weaker binding is caused by steric factors, but rather by electronic effects.

To evaluate the electronic effects that the phenylene-ethylene group has on the superstructures, we calculated the electrostatic potential and highest-occupied molecular orbital (HOMO) using the M06-HF functional. We observe from the electrostatic potential van der Waals surface (Figure 6a) that the naphthyl moiety on the disubstituted DEG-DNP is more

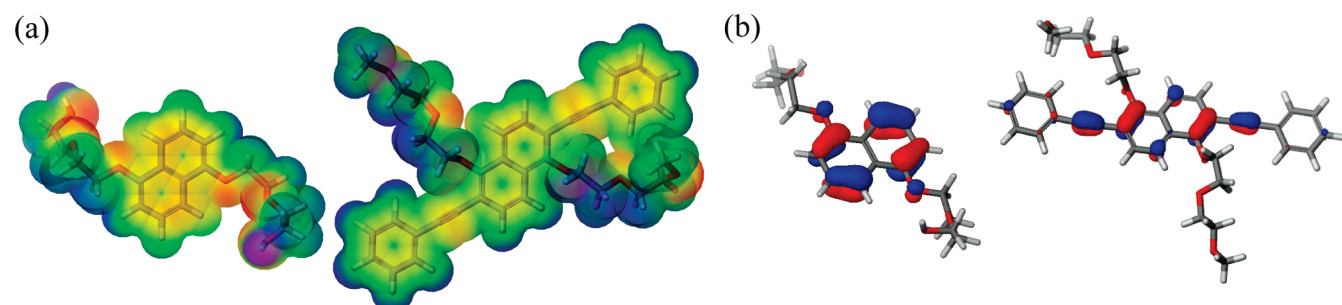


Figure 6. Graphical representation for the electronic differences between rigid and flexible thread components: (a) Electrostatic potential van der Waals surface plots for disubstituted DEG-DNP and **4** (color levels are equal for both superstructures). (b) Highest-occupied molecular orbital (HOMO) for DEG-DNP and **4**. The HOMO on DEG-DNP is localized at the DNP unit, whereas it is delocalized over the conjugated aromatic system on **4**.

negatively charged (shaded yellow) than in the case of **4** (shaded green). The partial negative charge of **4** is localized over the acetylenic groups (shaded orange), whereas the protons that are responsible for [C—H \cdots π] interactions are colored in blue (partially positive). By contrast, the stronger disubstituted DEG-DNP complex shows orange shading over the naphthyl ring and green shading on the 3, 4, 7, and 8 protons that play a crucial role in the binding. In addition, the HOMO (Figure 6b) of **4** is delocalized over the extended aromatic system and at 0.1 eV lower in energy, hence reducing the interaction with the high lying unoccupied orbitals on **CBPQT** $^{4+}$.

Conclusions

The crystal superstructures of the rigid HQ- and DNP-based model compounds **2** and **4**, which incorporate phenylacetylene units, and their binding behavior with the π -electron deficient tetracationic cyclophane, **CBPQT** \cdot 4PF₆, were investigated in order to understand the relationship between the rigidity and complex stabilities in their complexes. Increased rigidity in the compounds **2** and **4** reflected directly into their complexation stabilities with **CBPQT** \cdot 4PF₆. The binding abilities of both compounds **2** and **4** with **CBPQT** \cdot 4PF₆ are significantly decreased compared with those with the more flexible disubstituted DEG chain-containing dumbbell-shaped compounds. Both **2** and **4** were synthesized as model compounds for binding toward **CBPQT** $^{4+}$ based on a donor–acceptor recognition motif in a rigid framework. The crystal structures of their intermediate compounds **1** and **3**, as references for **2** and **4**, respectively, show centrosymmetric and S-shaped conformations achieved by a combination of intra- and intermolecular [C—H \cdots O] and [C—H \cdots π] interactions. In **2**, the structure has folded and twisted conformations caused by hydrogen-bonding network, [C—H \cdots π] interactions, and face-to-face [π — π] stacking interactions. In **4**, the structure is folded and perpendicular between aromatic rings by hydrogen-bonding network, [C—H \cdots π] interactions with no face-to-face [π — π] stacking interactions. Presumably, introducing rigidity has changed the environment of the [C—H \cdots O] interactions between **CBPQT** $^{4+}$ and these model compounds. Density functional theory with the newly developed M06-suite of density functionals has been used to show that the reduced binding of donor–acceptor complexes with rigidity in both the guest and the host is a consequence of the electronic (and not steric) factors that the phenylacetylene units impose upon the DNP ring system. Our theoretical investigations suggest that rigid groups that are not conjugated will exhibit increased binding by **CBPQT** $^{4+}$, similar to that experienced by DNP ring systems carrying flexible groups.

Acknowledgment. This work was supported by the Microelectronics Advanced Research Corporation (MARCO) and its Focus Center Research Program (FCRP), the Center on Functional Engineered NanoArchitectonics (FENA), and NSF (ECS-0609128). Computational facilities were funded by grants from ARO-DURIP and ONR-DURIP. We thank Dr. Saeed I. Khan for his assistance with a Bruker SMART CCD diffractometer at UCLA.

Supporting Information Available: ITC spectra (PDF) and crystallographic information in CIF format. This material is available free of charge via the Internet at <http://pubs.acs.org>.

References

- (a) Reddington, M. V.; Slawin, A. M. Z.; Spencer, N.; Stoddart, J. F.; Vicent, C.; Williams, D. J. *J. Chem. Soc., Chem. Commun.* **1991**, 630–634. (b) Ashton, P. R.; Brown, C. L.; Chrystal, E. J. T.; Goodnow, T. T.; Kaifer, A. E.; Parry, K. P.; Slawin, A. M. Z.; Spencer, N.; Stoddart, J. F.; Williams, D. J. *Angew. Chem., Int. Ed.* **1997**, 36, 2070–2072. (c) Ashton, P. R.; Spencer, N.; Stoddart, J. F.; Williams, D. J. *J. Chem. Soc., Chem. Commun.* **1994**, 181–184. (d) Amabilino, D. B.; Ashton, P. R.; Boyd, S. E.; Lee, J. Y.; Menzer, S.; Stoddart, J. F.; Williams, D. J. *Angew. Chem., Int. Ed.* **1997**, 36, 2070–2072. (e) Asakawa, M.; Ashton, P. R.; Dehaen, W.; L'abbé, G.; Menzer, S.; Nouwen, J.; Raymo, F. M.; Stoddart, J. F.; Tolley, M. S.; Toppet, S.; White, A. J. P.; Williams, D. J. *Chem.—Eur. J.* **1997**, 3, 772–787. (f) Asakawa, M.; Ashton, P. R.; Balzani, V.; Credi, A.; Hamers, C.; Mattersteig, G.; Montalti, M.; Shipway, A. N.; Spencer, N.; Stoddart, J. F.; Tolley, M. S.; Venturi, M.; White, A. J. P.; Williams, D. J. *Angew. Chem., Int. Ed.* **1998**, 37, 333–337. (g) Asakawa, M.; Ashton, P. R.; Balzani, V.; Brown, C. L.; Credi, A.; Matthews, O. A.; Newton, S. P.; Raymo, F. M.; Shipway, A. N.; Spencer, N.; Quick, A.; Stoddart, J. F.; Tolley, M. S.; White, A. J. P.; Williams, D. J. *Chem.—Eur. J.* **1999**, 5, 860–875. (h) Ashton, P. R.; Bravo, J. A.; Raymo, F. M.; Stoddart, J. F.; White, A. J. P.; Williams, D. J. *Eur. J. Org. Chem.* **1999**, 899–908. (i) Balzani, V.; Credi, A.; Mattersteig, G.; Matthews, O. A.; Raymo, F. M.; Stoddart, J. F.; Venturi, M.; White, A. J. P.; Williams, D. J. *J. Org. Chem.* **2000**, 65, 1924–1936. (j) Jeppesen, J. O.; Becher, J.; Stoddart, J. F. *Org. Lett.* **2002**, 4, 557–560. (k) Alcalde, E.; Perez-Garcia, L.; Ramos, S.; Stoddart, J. F.; White, A. J. P.; Williams, D. J. *Mendeleev Commun.* **2004**, 233–235. (l) Flood, A. H.; Stoddart, J. F.; Steuerman, D. W.; Heath, J. R. *Science* **2004**, 306, 2055–2056. (m) Liu, Y.; Flood, A. H.; Stoddart, J. F. *J. Am. Chem. Soc.* **2004**, 126, 9150–9151. (n) Liu, Y.; Saha, S.; Vignon, S. A.; Flood, A. H.; Stoddart, J. F. *Synthesis* **2005**, 3437–3445. (o) Deng, W.-Q.; Flood, A. H.; Stoddart, J. F.; Goddard III, W. A. *J. Am. Chem. Soc.* **2005**, 127, 15994–15995. (p) Jang, S. S.; Jang, Y. H.; Kim, Y.-H.; Goddard III, W. A.; Choi, J. W.; Heath, J. R.; Laursen, B. W.; Flood, A. H.; Stoddart, J. F.; Norgaard, K.; Bjornholm, T. *J. Am. Chem. Soc.* **2005**, 127, 14804–14816. (q) Liu, Y.; Flood, A. H.; Bonvallet, P. A.; Vignon, S. A.; Northrop, B.; Tseng, H.-R.; Jeppesen, J.; Huang, T. J.; Brough, B.; Baller, M.; Magonov, S.; Solares, S.; Goddard III, W. A.; Ho, C.-M.; Stoddart, J. F. *J. Am. Chem. Soc.* **2005**, 127, 9745–9759. (r) Choi, J. W.; Flood, A. H.; Steuerman, D. W.; Nygaard, S.; Braunschweig, A. B.; Moonen, N. N. P.; Laursen, B. W.; Luo, Y.; Delonno, E.; Peters, A. J.; Jeppesen, J. O.; Xu, K.; Stoddart, J. F.; Heath, J. R. *Chem.—Eur. J.* **2006**, 261–279. (s) Miljanic, O. Š.; Dichtel, W. R.; Mortezaei, S.; Stoddart, J. F. *Org. Lett.* **2006**, 8, 4835–4838. (t) Dichtel, W. R.; Miljanic, O. Š.; Spruell, J. M.; Heath, J. R.; Stoddart, J. F. *J. Am. Chem. Soc.* **2006**, 128, 10388–10390. (u) Northrop, B. H.; Kahn, S. I.; Stoddart, J. F. *Org. Lett.* **2006**, 8, 2159–2162. (v) Aprahamian, I.; Miljanic, O. Š.; Dichtel, W. R.; Isoda, K.; Yasuda, T.; Kato, T.; Stoddart, J. F. *Bull. Chem. Soc. Jpn.* **2007**, 80, 1856–1869. (w) Miljanic, O. Š.; Stoddart, J. F. *Proc. Natl. Acad. Sci. U.S.A.* **2007**, 104, 12966–12970. (x) Miljanic, O. Š.; Dichtel, W. R.; Khan, S. I.; Mortezaei, S.; Heath, J. R.; Stoddart, J. F. *J. Am. Chem. Soc.* **2007**, 129, 8236–8246. (y) Nygaard, S.; Leung, K. C.-F.; Aprahamian, I.; Ikeda, T.; Saha, S.; Laursen, B. W.; Kim, S.-Y.; Hansen, S. W.; Stein, P. C.; Flood, A. H.; Stoddart, J. F.; Jeppesen, J. O. *J. Am. Chem. Soc.* **2007**, 129, 960–970. (z) Yoon, I.; Miljanic, O. Š.; Benitez, D.; Khan, S. I.; Stoddart, J. F. *Chem. Commun.* **2008**, 4561–4563.
- (a) Ashton, P. R.; Odell, B.; Reddington, M. V.; Slawin, A. M. Z.; Stoddart, J. F.; Williams, D. J. *Angew. Chem., Int. Ed.* **1988**, 27, 1550–1553. (b) Ashton, P. R.; Goodnow, T. T.; Kaifer, A. E.; Reddington, M. V.; Slawin, A. M. Z.; Spencer, N.; Stoddart, J. F.; Vicent, C.; Williams, D. J. *Angew. Chem., Int. Ed.* **1989**, 28, 1396–1399. (c) Anelli, P. L.; Ashton, P. R.; Spencer, N.; Slawin, A. M. Z.; Stoddart, J. F.; Williams, D. J. *Angew. Chem., Int. Ed.* **1991**, 30, 1036–1039. (d) Ashton, P. R.; Brown, C. L.; Chrystal, E. J. T.; Goodnow, T. T.; Kaifer, A. E.; Parry, K. P.; Slawin, A. M. Z.; Spencer, N.; Stoddart, J. F.; Williams, D. J. *Angew. Chem., Int. Ed.* **1991**, 30, 1039–1042. (e) Ashton, P. R.; Brown, C. L.; Chrystal, E. J. T.; Parry, K. P.; Pietraszkiewicz, M.; Spencer, N.; Stoddart, J. F. *Angew. Chem., Int. Ed.* **1991**, 30, 1042–1045. (f) Anelli, P. L.; Ashton, P. R.; Ballardini, R.; Balzani, V.; Delgado, M.; Gandolfi, M. T.; Goodnow, T. T.; Kaifer, A. E.; Philip, D.; Pietraszkiewicz, M.; Prodi, L.; Reddington, M. V.; Slawin, A. M. Z.; Spencer, N.; Stoddart, J. F.; Vicent, C.; Williams, D. J. *J. Am. Chem. Soc.* **1992**, 114, 193–218. (g) Amabilino, D. B.; Ashton, P. R.; Brown, C. L.; Cordova, E.; Godinez, L. A.; Hayes, W.; Kaifer, A. E.; Philip, D.; Slawin, A. M. Z.; Spencer, N.; Stoddart, J. F.; Tolley, M. S.; Williams,

- D. J. *J. Am. Chem. Soc.* **1995**, *117*, 11142–11170. (i) Asakawa, M.; Brown, C. L.; Menzer, S.; Raymo, F. M.; Stoddart, J. F.; Williams, D. J. *J. Am. Chem. Soc.* **1997**, *119*, 2614–2627. (j) Bravo, A.; Raymo, F. M.; Stoddart, J. F.; White, A. J. P.; Williams, D. J. *Eur. J. Org. Chem.* **1998**, 2565–2571. (k) Matthews, O. A.; Raymo, F. M.; Stoddart, J. F.; White, A. J. P.; Williams, D. J. *New J. Chem.* **1998**, 1131–1134. (l) Asakawa, M.; Ashton, P. R.; Balzani, V.; Boyd, S. E.; Credi, A.; Mattersteig, G.; Menzer, S.; Montalti, M.; Raymo, F. M.; Ruffilli, C.; Stoddart, J. F.; Venturi, M.; Williams, D. J. *Eur. J. Org. Chem.* **1999**, 985–994. (m) Lau, J.; Nielsen, M. B.; Thorup, N.; Cava, M. P.; Becher, J. *Eur. J. Org. Chem.* **1999**, 3335–3341. (n) Ballardini, R.; Balzani, V.; Fabio, A. D.; Gandolfi, M. T.; Becher, J.; Lau, J.; Nielsen, M. B.; Stoddart, J. F. *New J. Chem.* **2001**, *25*, 293–298. (o) Alcalde, E.; Perez-Garcia, L.; Ramos, S.; Stoddart, J. F.; Vignon, S. A.; White, A. J. P.; Williams, D. J. *Mendeleev Commun.* **2003**, 100–102.
- (3) (a) Odell, B.; Reddington, M. V.; Slawin, A. M. Z.; Spencer, N.; Stoddart, J. F.; Williams, D. J. *Angew. Chem., Int. Ed.* **1988**, *27*, 1547–1550. (b) Asakawa, M.; Dehaen, W.; L’abbé, G.; Menzer, S.; Nouwen, J.; Raymo, F. M.; Stoddart, J. F.; Williams, D. J. *J. Org. Chem.* **1996**, *61*, 9591–9595. (c) Doddi, G.; Ercolani, G.; Mencarelli, P.; Piermattei, A. J. *Org. Chem.* **2005**, *70*, 3761–3764.
- (4) For molecular electronic devices (MEDs), see: (a) Collier, C. P.; Mattersteig, G.; Wong, E. W.; Luo, Y.; Beverly, K.; Sampaio, J.; Raymo, F. M.; Stoddart, J. F.; Heath, J. R. *Science* **2000**, *289*, 1172–1175. (b) Flood, A. H.; Peters, A. J.; Vignon, S. A.; Steuerman, D. W.; Tseng, H.-R.; Kang, S.; Heath, J. R.; Stoddart, J. F. *Chem.—Eur. J.* **2004**, *10*, 6558–6564. (c) DeIonno, E.; Tseng, H.-R.; Harvey, D. D.; Stoddart, J. F.; Heath, J. R. *J. Phys. Chem. B* **2006**, *110*, 7609–7612. (d) Green, J. E.; Choi, J. W.; Boukai, A.; Bunimovich, Y.; Johnston-Halpin, E.; DeIonno, E.; Luo, Y.; Sheriff, B. A.; Xu, K.; Shin, Y. S.; Tseng, H.-R.; Stoddart, J. F.; Heath, J. R. *Nature* **2007**, *445*, 414–417.
- (5) (a) Houk, K. N.; Menzer, S.; Newton, S. P.; Raymo, F. M.; Stoddart, J. F.; Williams, D. J. *J. Am. Chem. Soc.* **1999**, *121*, 1479–1487. (b) Raymo, F. M.; Barberger, M. D.; Houk, K. N.; Stoddart, J. F. *J. Am. Chem. Soc.* **2001**, *123*, 9264–9267.
- (6) Jeppesen, J. O.; Vignon, S. A.; Stoddart, J. F. *Chem.—Eur. J.* **2003**, *9*, 4611–4625.
- (7) (a) Leigh, D. A.; Wong, J. K. Y.; Dehez, F.; Zerbetto, F. *Nature* **2003**, *424*, 174–179. (b) Berna, J.; Leigh, D. A.; Lubomska, M.; Mendoza, S. M.; Perez, E. M.; Rudolf, P.; Teobaldi, G.; Zerbetto, F. *Nat. Mater.* **2005**, *4*, 704–710. (c) van Delden, R. A.; ter Wiel, M. K. J.; Pollard, M. M.; Vicario, J.; Koumura, N.; Feringa, B. L. *Nature* **2005**, *437*, 1337–1340. (d) Balzani, V.; Clemente-Léon, M.; Credi, A.; Ferrer, B.; Venturi, M.; Flood, A. H.; Stoddart, J. F. *Proc. Natl. Acad. Sci. U.S.A.* **2006**, *103*, 1178–1183. (e) Brough, B.; Northrop, B. H.; Schmidt, J. J.; Tseng, H.-R.; Houk, K. N.; Stoddart, J. F.; Ho, C.-M. *Proc. Natl. Acad. Sci. U.S.A.* **2006**, *103*, 8583–8588. (f) Kay, E. R.; Leigh, D. A.; Zerbetto, F. *Angew. Chem., Int. Ed.* **2007**, *46*, 72–191. (g) Serreli, V.; Lee, C. F.; Kay, E. R.; Leigh, D. A. *Nature* **2007**, *445*, 523–527. (h) Saha, S.; Stoddart, J. F. *Chem. Soc. Rev.* **2007**, *36*, 77–92. (i) Balzani, V.; Credi, A.; Venturi, M. *Nano Today* **2007**, *2*, 18–25. (j) Saha, S.; Leung, K. C.-F.; Nguyen, T. D.; Stoddart, J. F.; Zink, J. I. *Adv. Funct. Mater.* **2007**, *17*, 685–693. (k) Bath, J.; Turberfield, A. J. *Nat. Nanotechnol.* **2007**, *2*, 275–284.
- (8) (a) Jang, Y. H.; Goddard III, W. A. *J. Phys. Chem. B* **2006**, *110*, 7660–7665. (b) Ikeda, T.; Saha, S.; Aprahamian, I.; Leung, K. C. F.; Williams, A.; Deng, W. Q.; Flood, A. H.; Goddard III, W. A.; Stoddart, J. F. *Chem. Asian J.* **2007**, 76–93. (c) Jacob, T.; Blanco, M.; Goddard III, W. A. *J. Phys. Chem. C* **2007**, *111*, 2749–2758. (d) Kim, Y. H.; Goddard III, W. A. *J. Phys. Chem. C* **2007**, *111*, 4831–4837.
- (9) Benítez, D.; Tkatchouk, E.; Yoon, I.; Stoddart, J. F.; Goddard III, W. A. *J. Am. Chem. Soc.* **2008**, *130*, 14928–14929.
- (10) (a) Zhao, Y.; Truhlar, D. G. *Theor. Chem. Acc.* **2008**, *120*, 215–241. (b) Zhao, Y.; Truhlar, D. G. *Acc. Chem. Res.* **2008**, *41*, 157–167.
- (11) *Jaguar*, version 7.0; Schrödinger, LLC: New York, 2007.
- (12) Lauter, U.; Meyer, W. H.; Wegner, G. *Macromolecules* **1997**, *30*, 2092–2101.
- (13) Egbe, D. A. M.; Bader, C.; Klemm, E.; Ding, L.; Karasz, F. E.; Grummt, U.-W.; Birckner, E. *Macromolecules* **2003**, *36*, 9303–9312.
- (14) (a) Sonogashira, K.; Tohda, Y.; Hagihara, N. *Tetrahedron Lett.* **1975**, *50*, 4467–4470. (b) Takahashi, S.; Kuroyama, Y.; Sonogashira, K.; Hagihara, N. *Synthesis* **1980**, 627–630.
- (15) For accounts and reviews on [C–H \cdots π] interactions, see: (a) Nishio, M.; Umezawa, Y.; Hirota, M.; Takeuchi, Y. *Tetrahedron* **1995**, *51*, 8665–8701. (b) Umezawa, Y.; Tsuboyama, S.; Honda, K.; Uzawa, J.; Nishio, M. *Bull. Chem. Soc. Jpn.* **1998**, *71*, 1207–1213. (c) Nishio, M.; Hirota, M.; Umezawa, Y. *The [C–H \cdots π] Interaction. Evidence, Nature, and Consequences*; Wiley: New York, 1998.
- (16) (a) Ahbab, M.; Borthwick, A. D.; Hooper, J. W.; Millership, J. S.; Whalley, W. B.; Ferguson, G.; Marsh, F. C. *J. Chem. Soc., Perkin Trans. 1* **1976**, 1369–1376. (b) Lineberry, A. M.; Wheeler, K. A. *Acta Crystallogr., Sect. E* **2006**, *62*, o3870–o3872.
- (17) Li, H.; Powell, D. R.; Firman, T. K.; West, R. *Macromolecules* **1998**, *31*, 1093–1098.
- (18) Sanyal, N.; Lahti, P. M. *Cryst. Growth Des.* **2006**, *6*, 1253–1255.
- (19) For accounts and reviews on [π – π] stacking interactions, see: (a) Hunter, C. A.; Sanders, J. K. M. *J. Am. Chem. Soc.* **1990**, *112*, 5525–5534. (b) Hunter, C. A. *Angew. Chem., Int. Ed.* **1993**, *32*, 1584–1586. (c) Cozzi, F.; Siegel, J. S. *Pure Appl. Chem.* **1995**, *67*, 683–689. (d) Shetty, A. S.; Zhang, J.; Moore, J. S. *J. Am. Chem. Soc.* **1996**, *118*, 1019–1027.

CG801106H